Title

SnoN activates p53 directly to regulate aging and tumorigenesis

Journal

Aging Cell, 11(5)

ISSN

1474-9718

Authors

Pan, Deng

Zhu, Qingwei

Conboy, Michael J

et al.

Publication Date

2012-10-01

DOI

10.1111/j.1474-9726.2012.00857.x

Peer reviewed

Published in final edited form as:
Aging Cell. 2012 October ; 11(5): 902–911. doi:10.1111/j.1474-9726.2012.00857.x.

SnoN activates p53 directly to regulate aging and tumorigenesis

Deng Pan[#1,3], **Qingwei Zhu**[#1], **Michael J. Conboy**[2], **Irina M. Conboy**[2], and **Kunxin Luo**[1,*]
[1]Department of Molecular and Cell Biology, University of California, Berkeley, CA 94720

[2]Department of Bioengineering and QB3 University of California, Berkeley, CA 94720

[#] These authors contributed equally to this work.

Summary

We have identified SnoN as a direct activator of p53 to accelerate aging and inhibit tumorigenesis. SnoN has been shown previously to promote proliferation and transformation by antagonizing TGFβ signaling. We show that elimination of this TGFβ antagonistic activity of SnoN in vivo results in accelerated aging and resistance to tumorigenesis. The SnoN knockin mice display a shortened lifespan, decreased reproductivity, osteoporosis, reduced regenerative capacity and other aging phenotypes, similar to that found in mice expressing an active p53. These activities of SnoN rely on the ability of SnoN to activate p53. SnoN can bind directly to p53 and compete with Mdm2 for binding to p53, preventing p53 ubiquitination and degradation and additionally facilitating p53 acetylation and phosphorylation. SnoN also binds to p53 on the promoter of p53 responsive genes to promote transcription activation. This activation of p53 by SnoN is necessary for its anti-tumorigenic and progeria activities in vivo since elimination of one copy of p53 reverses the aging phenotypes and accelerates tumorigenesis. Thus, we have revealed a novel function of SnoN in regulating aging and tumorigenesis by directly activating p53.

Introduction

p53 is activated by various stress signals to coordinate cell cycle arrest, apoptosis, senescence and DNA repair processes (Vousden & Prives 2009). While activation of p53 serves as an effective mechanism to reduce cancer susceptibility, it also compromises longevity by accelerating aging (Rodier *et al*. 2007; Donehower 2009). Expression of a constitutively active p53 in mice protects the animal from tumorigenesis, at the same time accelerates aging (Tyner *et al*. 2002). Understanding the regulation of this pathway by

[*]To whom correspondence should be addressed: Department of Molecular and Cell Biology University of California 16 Barker Hall, MC3204 Berkeley, CA 94720 kluo@berkeley.edu Tel: 1-510-643-3183; Fax: 1-510-642-7038 .
[3]Current address: Department of Pathology, University of California, San Francisco, CA 94143

Author contributions: K.L designed research; D.P., Q.Z.and M.C. performed research; I.C. contributed new reagents/analytic tools; D.P., Q.Z. and K.L. analyzed data; and D.P., Q.Z. and K.L. wrote the paper.

The authors declare no conflict of interest.

Supporting information listing:

- Fig. S1: Aging phenotypes in SnoN knockin mouse.
- Fig. S2: Characterization of the interaction between SnoN and p53.
- Fig. S3: SnoN has a higher affinity for p53 than Mdm2.
- Fig. S4: Interactions between SnoN and p53 is required for SnoN-induced senescence.
- Supplemental Materials and Methods.

raw data of mouse survival plot (Fig. 1A)

intrinsic and extrinsic signals is therefore critical to address unsolved questions in senescence and cancer.

Regulation of p53 mainly occurs at post-transcriptional levels, in particular protein stability, and is primarily controlled by the Mdm2 E3 ubiqitin ligase that induces poly-ubiquitination and degradation of p53 (Kruse & Gu 2009). Mdm2 may further repress p53 transcription by forming a repressor complex with p53 on the promoter DNA. The stress signals induce stabilization of p53 by blocking the Mdm2-p53 interaction either through post-translational modification of p53 and Mdm2 or physical competition (Lu 2010). Phosphorylation and acetylation of p53 can further activate its transcriptional activity and facilitate recruitment of other transcription co-activators (Oren *et al*. 2002; Kruse & Gu 2009). Activation of p53 in response to cellular stresses also requires the PML protein. PML is essential for the formation of the PML nuclear bodies that allow recruitment of diverse proteins to the nuclear domain (Dellaire *et al*. 2006; Bernardi & Pandolfi 2007) and serve as a scaffold to increase the local concentrations of factors involved in p53 activation (Pearson *et al*. 2000; Pearson & Pelicci 2001). Loss of PML allows mouse embryo fibroblasts (MEF) to bypass senescence due to lack of p53 activation (Ferbeyre *et al*. 2000; de Stanchina *et al*. 2004).

We have recently identified SnoN as a novel upstream regulator of p53 to induce cellular senescence in response to oxidative stress. SnoN is a member of the Ski family of proteins (Nomura *et al*. 1989) and is ubiquitously expressed in all cell types and tissues (Deheuninck & Luo 2009; Jahchan & Luo 2010). Its expression can be induced during tissue morphogenesis (Jahchan *et al*. 2010), by injury (Mayoral *et al*. 2010) and upon stimulation with cytokines such as TGFβ (Zhu *et al*. 2005). SnoN is a potent negative regulator of TGFβ signaling by binding to the Smad proteins and repressing their transactivation activity (Deheuninck & Luo 2009). This ability to antagonize the growth inhibitory responses to TGFβ is likely responsible for the prooncogenic activity of SnoN (Wu *et al*. 2002; He *et al*. 2003). Indeed, reducing SnoN in breast and lung cancer cell lines reversed transformation in vitro and tumor growth in vivo, and re-introduction of WT but not the mutant SnoN lacking the Smad binding sites rescued this response (Zhu *et al*. 2007).

In an effort to uncover Smad-independent functions of SnoN, we generated a knockin mouse ($SnoN^{m/m}$) expressing a mutant SnoN defective in binding to the Smad proteins in the original *snoN* locus. Using MEF isolated from the knockin mice, we have shown that high levels SnoN can bind to PML and be recruited to the PML nuclear bodies where it upregulates p53 expression, leading to premature senescence (Pan *et al*. 2009). Consistent with this ability of SnoN to activate the PML-p53 tumor suppressor pathway, overexpression of SnoN inhibited oncogene-induced cellular transformation of MEF cells and significantly blocked chemical carcinogen-induced carcinogenesis carcinogenesis due likely to the accumulation of senescent cells in the $SnoN^{m/m}$ mice (Pan *et al*. 2009).

Two key unresolved questions are: 1) how does SnoN upregulate and activate p53 once it is recruited to the PML nuclear bodies? 2) What is the physiological function of the SnoN activation of p53? Since active p53 promotes aging, we predict that SnoN may also accelerate aging. In this report, we directly addressed these questions. Our studies have revealed a previously unidentified function of SnoN to promote premature aging. We have also determined the mechanism by which SnoN activates p53.

Results

The SnoN knockin mice display accelerated aging phenotypes

The SnoN knockin mouse ($SnoN^{m/m}$) expressing a mutant SnoN that contains point mutations altering the R-Smad and Smad4 binding sites (Fig. 1A). Our earlier study has

shown that this mutant SnoN protein (mSnoN) is defective in binding to the Smad proteins, and as a result of this, cells harboring this mSnoN display elevated Smad signaling activity as well as increased mSnoN protein levels (Pan *et al*. 2009). Using MEF isolated from the $SnoN^{m/m}$ mice that express a mutant SnoN defective in binding to the Smad proteins, we have uncovered a novel Smad-independent function of SnoN in inducing premature senescence through modulating p53 (Pan *et al*. 2009). During the routine maintenance and analysis of these mice, we noticed that these animals were very sensitive to environmental stress and often had difficulties getting pregnant or repairing wounds. Some of these phenotypes are often associated with the aging process. We therefore asked whether these mice display accelerated aging and whether they contain more senescent cells in vivo. To do so, we measured life span of a cohort of 43 $SnoN^{m/m}$ mice and 34 WT ($SnoN^{+/+}$) mice. 20.9% of $SnoN^{m/m}$ mice died within the first year as compared with only 8.8% of $SnoN^{+/+}$ mice (Fig. 1A). The median lifespan of $SnoN^{m/m}$ mice is around 75.3 weeks, about 25 weeks shorter than that of $SnoN^{+/+}$ mice (Fig. 1A). This decrease in lifespan is similar to that displayed by mice expressing an active p53 (Tyner *et al*. 2002). In the first few months after birth, the $SnoN^{m/m}$ mice did not show apparent gross abnormalities in development. Visible premature aging symptoms in $SnoN^{m/m}$ mice including growth retardation, grey hair appearance, body weight loss and kyphosis started to be detected after 6-month of age (Fig. 1B and 2A). Both male and female $SnoN^{m/m}$ mice stopped gaining body mass around 6- to 12–months of age, resulting in smaller body size (Fig. 1B). $SnoN^{m/m}$ mice also displayed decreased reproductive activity. The number of pups born to the matings of $SnoN^{m/m}$ mice with WT mice was significantly lower than that born to the mating of WT parents (Fig. 1C). Interestingly, when the metabolic activities including the oxygen consumption, generation of CO_2 and heat, and the general mobility were evaluated, no obvious difference was observed, suggesting that the accelerated aging observed in $SnoN^{m/m}$ mice does not involve changes in metabolic activities (data not shown).

Since there is no significant difference in bone density and structure between WT and $SnoN^{m/m}$ mice at 1-month of age (Fig. S1A), the marked kyphosis appeared in older $SnoN^{m/m}$ mice (Fig. 2A, left) suggested osteoporosis, an age-related bone degenerative disease common in both human and mouse (Watanabe & Hishiya 2005). Indeed when compared to age-matched WT mice, 18-month old $SnoN^{m/m}$ mice exhibited an overall reduction in bone density as shown by X-ray analysis (Fig. 2A, middle), a severe loss of honey comb-like bone structure inside the vertebrae as indicated by high-resolution MicroCT scan (Fig. 2A, top right), and a reduced cortical bone thickness and absence of trabecular bone as demonstrated by H&E stain of the tibias cross sections (Fig. 2A, bottom right). In addition to this early onset of osteoporosis, the skin of $SnoN^{m/m}$ mice also showed signs of prematured aging. H&E staining of dorsal skin sections of 12 month-old $SnoN^{m/m}$ mice revealed a significant decrease in the thickness of subcutaneous adipose layer, but not the dermal layers, when compared to that of age-matched WT skin. These differences were not detected at 4-month of age, again suggesting an aging process (Fig. 2B). The $SnoN^{m/m}$ mice also showed a markedly reduced hair regrowth activities (Fig. 2C). Thus, the SnoN knockin mice exhibit premature aging in multiple organs.

Aged animals often exhibited reduced regenerative activities. We therefore performed muscle injury and regeneration assay in age-matched $SnoN^{+/+}$ and $SnoN^{m/m}$ mice. 12-month old mice were subjected to injury by cardiotoxin-1 injection. Satellite cells (muscle stem cells) were isolated, and their ability to differentiate into myoblasts in vitro were analyzed by the expression of myogenic markers Desmin and MyoD (Brack *et al*. 2008). Satellite cells from injuried $SnoN^{m/m}$ muscles expressed a higher level of p15, p16 and p27 than that in $SnoN^{+/+}$ cells (Fig. 2D, left), but this difference was not detected in cells from uninjured mice (Fig. S1B). Consistent with this, these $SnoN^{m/m}$ satellite cells displayed moderately reduced proliferation (Fig. S1C). Importantly, the $SnoN^{m/m}$ satellite cells displayed a

markedly reduced myogenic ability with much less Desmin-positive cells than the $SnoN^{+/+}$ culture (Fig. 2D, right). The expression levels of Desmin and MyoD were also decreased significantly in cells differentiated from $SnoN^{m/m}$ satellite cells than that derived from the $SnoN^{+/+}$ cells (Fig. S1D). This reduced proliferation and differentiation of the $SnoN^{m/m}$ muscle stem cells were only observed in aged mice but not in mice of 1-6-month of age (Fig. S1D). Thus, muscle stem/progenitor cells from the $SnoN^{m/m}$ have a decreased regenerative potential.

Consistent with this accelerated aging, an increased number of senescent cells were observed in skin sections from $SnoN^{m/m}$ mice as evidenced by the marked increase in the level of SA-β–Gal (Fig. 2E) and $p19^{ARF}$ (Fig. S1E), two markers of senescence. Similarly, kidney sections from 18-month-old $SnoN^{m/m}$ mice also contained more senescent and apoptotic cells (Fig. S1F and data not shown). Taken together, our analyses indicate that the $SnoN^{m/m}$ mice showed shortened lifespan and accelerated aging, most likely due to enhanced senescence and apoptosis.

SnoN binds to p53 directly

We have shown before that $SnoN^{m/m}$ MEF cells displayed elevated p53 expression and premature senescence (Pan *et al*. 2009). Since hyperactive p53 has been shown to accelerate aging (Tyner *et al*. 2002), we asked whether tissues from the $SnoN^{m/m}$ mice may show heightened p53 expression. Indeed, p53 expression is elevated in skin (Fig. 2F) and kidney (Fig. S1G) of $SnoN^{m/m}$ mice when compared to age-matched WT mice by both western blotting and immunohistochemical staining, and this increase is more pronounced in aged animals (Fig. 2F, left). In addition, these tissues also displayed elevated levels of SnoN protein (Fig. S1H), as expected due to a lack of Smad-induced degradation. This elevated SnoN protein is likely to be responsible for the increased p53 expression in aging tissues.

In our earlier study, we have shown that high levels of SnoN can be recruited to the PML nuclear bodies to upregulate p53 expression in an Smad-independent manner (Pan *et al*. 2009). However, how SnoN upregulates p53 in PML nuclear bodies is not clear. We first test the possibility that SnoN may physically interact with p53 to promote its stabilization and activation. To do this, Flag-tagged p53 was transfected into 293T cells together with HA-SnoN and isolated by immunoprecipitation with anti-Flag, and p53-bound SnoN was detected by western blotting with anti-HA. As shown in Fig. 3A, SnoN can bind to p53 readily when overexpressed, and this interaction was not affected by the presence of the transfected PML. Consistent with this, mutant SnoN (Δ322-366) defective in binding to PML could bind to p53 as well as WT SnoN when overexpressed (Fig. 3B). In a GST-pull down assay, recombinant SnoN purified from bacteria could be pulled down together with GST-p53 but not with GST alone (Fig. 3C), suggesting that the SnoN-p53 interaction is direct. To determine whether this interaction also occurs at the endogenous level, MEF cells were treated with H_2O_2 (to induce p53), and the SnoN-p53 interaction was examined by co-immunoprecipitation assay. As shown in Fig. 3D, endogenous p53 readily interacts with SnoN. In addition, PML could also be detected in the SnoN immune complex, as shown before (Pan *et al*. 2009). When the PML level was reduced by specific shRNA, p53 expression was decreased dramatically (Fig. 3D), confirming that PML is required for p53 stabilization. Blocking the proteasome-mediated degradation with MG132, a proteasome inhibitor, in these shPML-expressing cells stabilized p53 expression, and SnoN was found to complex with p53 (Fig. 3D). This result suggests that PML is mainly required for stabilization of p53 and recruits both SnoN and p53 to the PML bodies, but is not directly involved in the SnoN-p53 interaction. In addition, binding of SnoN to PML is independent of p53. In $p53^{-/-}$ MEFs, SnoN co-localized with PML as efficiently as in WT cells (Fig.

S2A), suggesting that binding of SnoN to PML and localization of SnoN to PML bodies are upstream of the p53-SnoN interaction.

The interaction between SnoN and p53 is not unique to fibroblasts. In nonimmortalized human normal mammary epithelia cells (the 184 cells), SnoN could also bind to p53 (Fig. S2B). Again in the absence of PML, when p53 was stabilized with MG132, endogenous p53 bound to SnoN readily (Fig. S2B). Thus, SnoN can interact with p53 in both epithelial and fibroblast cells.

Mapping of p53 binding site in SnoN

We next mapped the residues or domains in SnoN that are required for binding to p53 using various SnoN mutants in a co-immunoprecipitation assay. p53 bound to the N-terminal portion SnoN (residue 1-366), but not to the C-terminal fragment (residues 367-684) (Fig. S2C). A small deletion of residues 255 to 258 in SnoN completely abolished the binding to p53 (Fig. 3E), but did not affect the binding of SnoN to Smads or PML (Fig. S2D-E) or the ability of SnoN to repress TGFβ induced transcription (Fig. S2F). This suggests that residues required for binding to p53 did not overlap with those for binding to PML and Smads.

Binding of SnoN to p53 is required for stabilization of p53

Previously we have shown that high levels of SnoN upregulate p53 expression, and this is critical for SnoN-induced senescence. To determine whether binding of p53 to SnoN causes stabilization of p53, a pulse-chase assay was performed to compare the half-life of SnoN-bound p53 with that of free p53. As reported before, in the absence of stress signals, p53 has a half-life shorter than 30 min (Fig. 4A). In contrast, the half-life of SnoN-bound p53 was significantly lengthened to at least 90 min. Overexpression of PML together with p53 and SnoN did not further stabilize p53. In the same cells, the half-life of SnoN was not affected by the expression of p53 or p53 plus PML (Fig. S3A). Consistent with the requirement of SnoN-p53 binding in p53 stabilization, the SnoN mutant (Δ255-258) defective in binding to p53 failed to stabilize p53 (Fig. 4B).

SnoN competes with Mdm2 for binding to p53

The half-life of p53 is tightly controlled by the Mdm2 E3 ubiquitin ligase. Dissociation of Mdm2 from p53 is essential for the stabilization and activation of p53 in response to cellular stress. To determine how SnoN binding stabilizes p53, we compared the association of Mdm2 with p53 in the presence or absence of SnoN. When cells were transfected with a fixed amount of Mdm2, p53 and increasing amounts of SnoN, Mdm2 was gradually competed away from p53 by the increased amount of SnoN (Fig. 4C). In the reverse experiment with a fixed amount of SnoN and increasing amounts of Mdm2, the SnoN-p53 complex was not affected by Mdm2 (Fig. 4C). This suggests that SnoN has a higher affinity for p53 than Mdm2. This is further confirmed in an in-vitro binding experiment using bacterially expressed recombinant GST-p53, Mdm2 and SnoN. When GST-p53 and recombinant Mdm2 were incubated with increased amount of recombinant SnoN, the SnoN-p53 complex increased while the Mdm2-p53 complex was significantly decreased (Fig. 4D). Similarly, in the reverse experiment with a fixed amount of SnoN and increased amounts of Mdm2, Mdm2 had no effect on the SnoN-p53 complex (Fig. S3B).

SnoN may compete with Mdm2 for binding to p53 through two possible mechanisms. First, the SnoN binding site in p53 may overlap with that of Mdm2. To test this, a p53 mutant, L14Q/F19S, defective in binding to Mdm2 but still retaining the transcription activity was examined for its ability to bind to SnoN. Interestingly, this p53 mutant also failed to bind to SnoN (Fig. 4E), suggesting that SnoN may bind to the same site in p53 as Mdm2.

SnoN may also regulate the post-translational modification of p53, for example acetylation or phosphorylation, which is known to reduce the affinity of p53 for Mdm2. To test this, SnoN-bound p53 was isolated from cells co-transfected with Flag-SnoN with anti-Flag, and free-p53 isolated from the SnoN-depleted cells with anti-p53. The acetylation and phosphorylation (Ser 15) of the SnoN-bound p53 were compared to that of free p53. As shown in Fig. 4F, SnoN-bound p53 clearly showed elevated acetylation and phosphorylation, suggesting that SnoN may also facilitate p53 modification. Although SnoN-bound p53 is acetylated and phoshporylated, these modifications are not required for binding of p53 to SnoN. The p53 (8R) mutant lacking all known acetylation Lysine residues and p53 (S15A) mutant both bound to SnoN to the same extent as WT p53 (Fig. 4G). Thus, SnoN may also bind to p53 to promote its acetylation and phosphorylation.

SnoN competes with Mdm2 for binding to the p53 responsive promoter DNA

Mdm2 not only regulates p53 degradation but also represses its transcriptional activity at the promoter DNA (Kruse & Gu 2009). Since SnoN competes with Mdm2 for binding to p53, it may also release the transcriptional repression by Mdm2 at the p53 responsive promoters. To test this, we examined recruitment of SnoN to the p53 responsive element in the $p21^{CIP1}$ promoter by chromatin immunoprecipitation (ChIP) assay. The $p21^{CIP1}$ promoter contains two p53 responsive elements located at −2.9 kb (RE1) and −1.9 kb (RE2) upstream of the transcription initiation site (el-Deiry *et al*. 1995). It also contains a TGFβ/Smad responsive element (SBE) at approximately −2.1 kb position (Seoane *et al*. 2004) (Fig. 5A). We examined binding of SnoN and Mdm2 to the RE1 region and also to the SBE region as a control. SnoN was found to bind to RE1, but only upon treatment of cells with H_2O_2 that induces p53 expression (Fig. 5A, right). This suggests that binding of SnoN to RE1 may be p53-dependent. In contrast, binding of SnoN to the SBE region was detected both in the presence and absence of p53 (Fig. 5A, right), confirming that this binding is p53 independent. To further confirm the p53-dependent nature of SnoN binding to RE1, the SnoN mutant (Δ255-258) defective in binding to p53 failed to bind to RE1 (Fig. 5B). Moreover, in $p53^{-/-}$ cells, even WT SnoN failed to be detected at the RE1 site (Fig. 5B). Thus, SnoN is recruited to the p53 responsive element through its association with p53.

To determine whether SnoN could release Mdm2 from the promoter DNA, binding of Flag-Mdm2 to RE1 was examined in the absence or presence of HA-SnoN. In the absence of SnoN, Mdm2 can be found to bind to RE1 (Fig. 5C). However, this binding was dramatically decreased when SnoN was present and bound to RE1 (Fig. 5C). This indicates that SnoN can displace Mdm2 from the promoter DNA of p53 responsive genes.

SnoN activates p53-dependent transcription

We next examined the effects of SnoN on p53-dependent transcription using a p21 promoter-driven luciferase reporter assay in $p53^{-/-}$ MEF cells. Expression of WT p53 significantly induced p21 transcription (Fig. 5D). Since p21 promoter is also induced by TGFβ/Smad pathway through the SBE site, and SnoN can potentially repress p21 transcription through antagonizing the Smads, thus complicating the interpretation of our assay, the mSnoN mutant defective in Smad binding was employed for this experiment. Expression of mSnoN alone had no effect on p21 transcription in $p53^{-/-}$ cells. However, p53-dependent transcription was clearly enhanced by co-expression of mSnoN (Fig. 5D). As reported previously, Mdm2 inhibited p53-dependent transcription. Consistent with the ability of SnoN to block the Mdm2/p53 interaction, mSnoN could significantly rescue p53-dependent transcription in the presence of Mdm2 (Fig. 5D).

The SnoN/p53 interaction is required for premature senescence

We have shown before that high levels of SnoN induced premature senescence of MEF in a p53-dependent manner (Pan *et al*. 2009). To determine whether the interaction of SnoN and p53 is required for this premature senescence, SnoN Δ255-258 defective in binding to p53 was introduced into primary MEF cells at P3. When expressed at similar level as WT SnoN, SnoN Δ255-258 failed to stabilize p53 and did not induce senescence (Fig. 6A). This SnoN still binds to PML, indicating that interaction of SnoN with PML is necessary but not sufficient for activation of p53 and induction of senescence and that interaction of SnoN with p53 is critical for this response.

The anti-oncogenic activity of SnoN is dependent on its interaction with p53

Next we determined whether the SnoN-p53 interaction is required for the anti-oncogenic function of SnoN in a MEF transformation assay. We have shown previously that high levels of SnoN inhibited oncogene-induced transformation of MEF, acting as a tumor suppressor (Pan *et al*. 2009). However in the absence of p53, SnoN could function as an oncogene to induce transformation by antagonizing the growth inhibitory activity of TGFβ. To determine whether elimination of the SnoN-p53 interaction disrupts the anti-oncogenic activity of SnoN to allow its oncogenic activity to be manifested, we introduced SnoN Δ255-258 into WT MEF cells together with the active Ras. The control experiment confirmed that p53 activation was abolished when the interaction between SnoN and p53 or PML was disrupted (Fig. 6B, right). While WT SnoN could not induce transformation of MEF cells in conjunction with the active Ras, SnoN Δ255-258 readily transformed MEF together with Ras (Fig. 6B, left). Moreover, overexpression of SnoN Δ255-258 alone in $p53^{-/-}$ MEF is sufficient to transform these cells (Fig. 6C). Thus, disrupting the SnoN-p53 interaction converts SnoN into an oncogene, and this suggests that interaction of SnoN with p53 is critical for its anti-oncogenic function in cells.

p53 is required for the anti-tumorigenic and progeria activity of SnoN in vivo

We have shown before that $SnoN^{m/m}$ mice are resistant to chemical-induced carcinogenesis, due possibly to p53-dependent senescence triggered by high levels of the SnoN protein (Pan *et al*. 2009). If elevated p53 in the $SnoN^{m/m}$ mice is indeed responsible for the resistance to tumorigenesis, reducing p53 level in these mice should restore tumor growth. We therefore crossed the $SnoN^{m/m}$ mice with $p53^{-/-}$ mice to generate $SnoN^{m/m}p53^{+/-}$ mice that expressed reduced level of p53. Mice were administered with one dose of DMBA followed by twice weekly treatment of TPA for 30 weeks, and development of papillomas was monitored. As shown before, the $SnoN^{m/m}$ mice displayed a greatly reduced ability to form papillomas when compared to $SnoN^{+/+}$ or $p53^{+/-}$ mice (Fig. 6D-6F). Interestingly, loss of one allele of p53 completely restored tumor growth. The $SnoN^{m/m}p53^{+/-}$ mice started to developed tumors after 8-week treatment, and papilloma development was observed in all $SnoN^{m/m}p53^{+/-}$ mice, similar to what was observed for $SnoN^{+/+}$ or $p53^{+/-}$ mice (Fig. 6D and 6E). More importantly, unlike that from the $SnoN^{m/m}$ mice, tumors from the $SnoN^{m/m}p53^{+/-}$ mice continued to grow to greater than 10 mm in diameter (Fig. 6F). When tumors harvested from these mice were examined for the presence of senescence responses, no senescent signals could be detected, in clear contrast from those from $SnoN^{m/m}$ mice that exhibited significant numbers of senescent cells (Fig. 6H and S4). Consistent with these, a high level of p53 was only detected in tumors from the $SnoN^{m/m}$ mice but not in those from $SnoN^{m/m}p53^{+/-}$ or $SnoN^{+/+}$ mice (Fig. 6G). These results indicate that p53 is required for the anti-oncogenic activity of SnoN in vivo. Interestingly, delection of one copy of p53 also rescued some of the premature aging phenotypes. The defective hair regrowth activity, reduced cortical bone thickness and trabecular bone structure as well as decreased body mass found in the $SnoN^{m/m}$ mice were all significantly rescued in the $SnoN^{m/m}p53^{+/-}$ mice

(Fig. 6I-J and data not shown). Thus, the ability of SnoN to activate p53 is a major contributor to its anti-oncogenic and progeria activity.

Discussion

We have established SnoN as a direct activator of p53 by competing with Mdm2 for binding to p53 both off and on promoter DNA, leading to p53 stabilization and activation. This ability of SnoN to activate p53 and induce cell senescence is not only responsible for its anti-tumorigenic activity, but also results in accelerated aging. Knockin mice expressing a form of SnoN that are accumulated to a high level are resistant to chemical carcinogen-induced tumorigenesis, more sensitive to environmental stress and display premature aging in a p53-dependent manner, consistent with the model that SnoN exerts its effects on tumor suppression and aging through activating p53. Thus, in adult cells, SnoN is not just an important negative regulator of TGFβ signaling, but plays a much broader role in co-ordinate the cellular stress responses by activating p53 to regulate cell cycle arrest, senescence and apoptosis.

SnoN likely induced p53 activation in the PML nuclear bodies. PML NBs contain many enzymes responsible for p53 modification and threfore are considered a regulation center for p53 in various stress responses. It is required for p53 stabilization and activation (Pearson & Pelicci 2001; Dellaire *et al*. 2006). Although not required for the direct SnoN-p53 interaction, PML NBs likely provide a scaffold to increase the local concentrations of SnoN and p53 to facilitate their interaction and for further post-transcriptional modifications and activation of p53 (Bernardi & Pandolfi 2007). Once SnoN-bound p53 is fully activated, this SnoN-p53 complex is then released from the PML NBs and localize to the promoter regions of p53 target genes, where they can activate transcription.

Consistent with SnoN activtion of p53, the accelerated aging phenotype found in the $SnoN^{m/m}$ mice is very similar to that observed in mice expressing a hyperactive p53, including a similarly shortened longevity, osteoporosis, reduced subcutaneous adipose tissue, decrease in hair regrowth and wound healing, and reduced tolerance to stresses (Tyner *et al*. 2002; Maier *et al*. 2004). It is worth noting that several mouse strains expressing an extra copy of WT p53 do not display premature aging phenotypes (Garcia-Cao *et al*. 2002), suggesting that p53 activation is crucial for the aging activity. The apparent progeria phenotypes observed in the $SnoN^{m/m}$ mice therefore support our model that SnoN not only induce p53 stabilization but also p53 activation. Furthermore, elimination of one copy of p53 from the $SnoN^{m/m}$ mice abolished the cancer resistance and many premature aging phenotypes, again indicating that these phenotypes are dependant on the activity of p53. It should be noted that although one p53 allele was detected in the $SnoN^{m/m}$ $p53^{+/-}$ mice, the p53 protein level was not readily detected in tumors from these mice, suggesting that the remaining p53 allele might be inactivated in these tumors. This inactivation of the remaining p53 allele could contribute to the complete lack of cancer resistance in the $SnoN^{m/m}$ $p53^{+/-}$ mice.

Unlike the $SnoN^{m/m}$ mice, the $SnoN^{-/-}$ mice did not display most of the aging phenotypes, suggesting that the closely related Ski protein did not compensate for the lack of SnoN. In addition, since the $SnoN^{-/-}$ mice also display elevated Smad signaling, the lack of aging phenotypes indicates that the elevated Smad activity is not a major contributor to aging. This is further supported by in vitro senescence assays where reducing Smad2/3 had no effect on premature senescence of $SnoN^{m/m}$ MEF (Pan *et al*. 2009). However, we cannot completely rule out the possibility that Smad signaling may contribute to some of the phenotypes. p53 has been shown previously to partner with Smad2 to form transcription complexes on DNA, and this interaction is required for Smad-dependent developmental events in Xenopus

embryos (Cordenonsi *et al*. 2003; Atfi & Baron 2008). Although this crosstalk has not been shown to affect p53 activity, we cannot exclude the possibility that some of the observed aging phenotypes of the $SnoN^{m/m}$ mice are the result of coordinated actions of active p53 and elevated Smad signaling.

Taken together, our study showed that SnoN may serve as an important anti-cancer defense mechanism at times of prolonged cellular stress and tissue injury by integrates various cellular stress signals to the p53 anti-tumorigenic pathway. These stress responses protect the organism against cancer but do so at the price of accelerated aging. An important future question is whether SnoN is also involved in the human aging process. Although no report implicating SnoN or its mutation in human aging syndromes has been published, given our result linking SnoN with oxidative stress-induced p53 activation, it is likely that SnoN may play a role in the natural human aging process.

Experimental Procedures

Immunoprecipitation and Western Blotting

Immunoprecipitation and western blotting were carried out as described previously (Zhu *et al*. 2007). For pulse-chase assays, cells were pulsed with 0.4 mCi/ml ^{35}S-express (Roche) for 30 min and chased as described previously (Stroschein *et al*. 1999).

GST pull-down

1.5 μg GST-p53 immobilized on the glutathione Sepharose were incubated with 2 μg recombinant SnoN for 1 hour at 4°C. For competition experiments, 1.5 μg immobilized GST-p53 were incubated with indicated amounts of recombinant SnoN or Mdm2. p53-bound proteins were eluted by boiling in SDS and detected by western blotting.

SA-β-gal staining and Immunofluorescence

The senescence detection kit (Calbiochem) was employed to stain the senescent cells and 6 μm-thick frozen tissue sections as described (Pan *et al*. 2009).

Immunofluorescence was carried out as described in Supplemental Materials.

For BrdU assay, cells were incubated with medium containing 0.1mg/ml BrdU (Roche) for 6 hours and stained with anti-BrdU working solution (Roche) followd by Alexa Fluor 488-conjugated goat anti-mouse-IgG (Invitrogen).

Chromatin immunoprecipitation (ChIP) assay

Transcription factor-associated DNA fragments were isolated by ChIP as described previously (Zhu *et al*. 2005) using the primer pairs described in Supplemental Materials.

Skin carcinogenesis assay and Soft-agar assay

The two-step skin carcinogenesis assay and soft-agar assay were carried out as described previously (Pan *et al*. 2009).

Analysis of aging phenotypes

The $SnoN^{m/m}$ and $SnoN^{+/+}$ littermates were monitored weekly for gross differences in appearance, weighted monthly from 0-18 months and various tissues collected at 4-18 months of age for histology analysis. For the hair regrowth assay, the lower dorsal surfaces were shaved, and the rate of hair regrowth was assessed one month later. Muscle injury and

regeneration assay and in vitro differentiation of satellite cells were performed as described previously (Carlson *et al*. 2008). More details can be found in Supplemental Materials.

Statistical analysis

Paired and unpaired Student's t test and Mann-Whitney U-test were used for statistical analysis. Quantitative data are presented as the mean ± SEM. Values of $p \leq 0.05$ were considered statistically significant.

Supplementary Material

Refer to Web version on PubMed Central for supplementary material.

Acknowledgments

We thank Drs. Astar Winoto, Xinbin Chen and Wei Gu for various p53 mutants and Mdm2 constructs; Dr. Sunita Ho, Sabra Djomehri and Mel Abulencia at UCSF for X-rays and microCT services; Dr. David Raulet for $p53^{-/-}$ mice; Drs. Hitoshi Nishimura and Dragana Cado for generating the $SnoN^{m/m}$ mice. We are grateful to Dr. Judy Campisi for discussions and helpful suggestions. This work was supported by NIH RO1 CA101891 and Philip Morris External Research Program grant 019016 to K. Luo.

References

Atfi A, Baron R. p53 brings a new twist to the Smad signaling network. Sci Signal. 2008; 1:pe33. [PubMed: 18594115]

Bernardi R, Pandolfi PP. Structure, dynamics and functions of promyelocytic leukaemia nuclear bodies. Nat Rev Mol Cell Biol. 2007; 8:1006–1016. [PubMed: 17928811]

Brack AS, Conboy IM, Conboy MJ, Shen J, Rando TA. A temporal switch from notch to Wnt signaling in muscle stem cells is necessary for normal adult myogenesis. Cell stem cell. 2008; 2:50–59. [PubMed: 18371421]

Carlson ME, Hsu M, Conboy IM. Imbalance between pSmad3 and Notch induces CDK inhibitors in old muscle stem cells. Nature. 2008; 454:528–532. [PubMed: 18552838]

Cordenonsi M, Dupont S, Maretto S, Insinga A, Imbriano C, Piccolo S. Links between tumor suppressors: p53 is required for TGF-beta gene responses by cooperating with Smads. Cell. 2003; 113:301–314. [PubMed: 12732139]

de Stanchina E, Querido E, Narita M, Davuluri RV, Pandolfi PP, Ferbeyre G, Lowe SW. PML is a direct p53 target that modulates p53 effector functions. Mol Cell. 2004; 13:523–535. [PubMed: 14992722]

Deheuninck J, Luo K. Ski and SnoN, potent negative regulators of TGF-beta signaling. Cell Res. 2009; 19:47–57. [PubMed: 19114989]

Dellaire G, Ching RW, Ahmed K, Jalali F, Tse KC, Bristow RG, Bazett-Jones DP. Promyelocytic leukemia nuclear bodies behave as DNA damage sensors whose response to DNA double-strand breaks is regulated by NBS1 and the kinases ATM, Chk2, and ATR. J Cell Biol. 2006; 175:55–66. [PubMed: 17030982]

Donehower LA. Using mice to examine p53 functions in cancer, aging, and longevity. Cold Spring Harb Perspect Biol. 2009; 1:a001081. [PubMed: 20457560]

el-Deiry WS, Tokino T, Waldman T, Oliner JD, Velculescu VE, Burrell M, Hill DE, Healy E, Rees JL, Hamilton SR, et al. Topological control of p21WAF1/CIP1 expression in normal and neoplastic tissues. Cancer Res. 1995; 55:2910–2919. [PubMed: 7796420]

Ferbeyre G, de Stanchina E, Querido E, Baptiste N, Prives C, Lowe SW. PML is induced by oncogenic ras and promotes premature senescence. Genes Dev. 2000; 14:2015–2027. [PubMed: 10950866]

Garcia-Cao I, Garcia-Cao M, Martin-Caballero J, Criado LM, Klatt P, Flores JM, Weill JC, Blasco MA, Serrano M. "Super p53" mice exhibit enhanced DNA damage response, are tumor resistant and age normally. EMBO J. 2002; 21:6225–6235. [PubMed: 12426394]

He J, Tegen SB, Krawitz AR, Martin GS, Luo K. The transforming activity of Ski and SnoN is dependent on their ability to repress the activity of Smad proteins. J Biol Chem. 2003; 278:30540–30547. [PubMed: 12764135]

Jahchan NS, Luo K. SnoN in mammalian development, function and diseases. Curr Opin Pharmacol. 2010; 10:670–675. [PubMed: 20822955]

Jahchan NS, You YH, Muller WJ, Luo K. Transforming growth factor-beta regulator SnoN modulates mammary gland branching morphogenesis, postlactational involution, and mammary tumorigenesis. Cancer Res. 2010; 70:4204–4213. [PubMed: 20460516]

Kruse JP, Gu W. Modes of p53 regulation. Cell. 2009; 137:609–622. [PubMed: 19450511]

Lu X. Tied up in loops: positive and negative autoregulation of p53. Cold Spring Harb Perspect Biol. 2010; 2:a000984. [PubMed: 20452957]

Maier B, Gluba W, Bernier B, Turner T, Mohammad K, Guise T, Sutherland A, Thorner M, Scrable H. Modulation of mammalian life span by the short isoform of p53. Genes Dev. 2004; 18:306–319. [PubMed: 14871929]

Mayoral R, Valverde AM, Llorente Izquierdo C, González-Rodríguez A, Boscá L, Martín-Sanz P. Impairment of transforming growth factor beta signaling in caveolin-1-deficient hepatocytes: role in liver regeneration. J Biol Chem. 2010; 285:3633–3642. [PubMed: 19966340]

Nomura N, Sasamoto S, Ishii S, Date T, Matsui M, Ishizaki R. Isolation of human cDNA clones of ski and the ski-related gene, sno. Nucleic Acids Res. 1989; 17:5489–5500. [PubMed: 2762147]

Oren M, Damalas A, Gottlieb T, Michael D, Taplick J, Leal JF, Maya R, Moas M, Seger R, Taya Y, Ben-Ze'Ev A. Regulation of p53: intricate loops and delicate balances. Ann N Y Acad Sci. 2002; 973:374–383. [PubMed: 12485897]

Pan D, Zhu Q, Luo K. SnoN functions as a tumour suppressor by inducing premature senescence. Embo J. 2009; 28:3500–3513. [PubMed: 19745809]

Pearson M, Carbone R, Sebastiani C, Cioce M, Fagioli M, Saito S, Higashimoto Y, Appella E, Minucci S, Pandolfi PP, Pelicci PG. PML regulates p53 acetylation and premature senescence induced by oncogenic Ras. Nature. 2000; 406:207–210. [PubMed: 10910364]

Pearson M, Pelicci PG. PML interaction with p53 and its role in apoptosis and replicative senescence. Oncogene. 2001; 20:7250–7256. [PubMed: 11704853]

Rodier F, Campisi J, Bhaumik D. Two faces of p53: aging and tumor suppression. Nucleic Acids Res. 2007; 35:7475–7484. [PubMed: 17942417]

Seoane J, Le HV, Shen L, Anderson SA, Massague J. Integration of Smad and forkhead pathways in the control of neuroepithelial and glioblastoma cell proliferation. Cell. 2004; 117:211–223. [PubMed: 15084259]

Stroschein SL, Wang W, Zhou S, Zhou Q, Luo K. Negative feedback regulation of TGF-beta signaling by the SnoN oncoprotein. Science. 1999; 286:771–774. [PubMed: 10531062]

Tyner SD, Venkatachalam S, Choi J, Jones S, Ghebranious N, Igelmann H, Lu X, Soron G, Cooper B, Brayton C, Hee Park S, Thompson T, Karsenty G, Bradley A, Donehower LA. p53 mutant mice that display early ageing-associated phenotypes. Nature. 2002; 415:45–53. [PubMed: 11780111]

Vousden KH, Prives C. Blinded by the Light: The Growing Complexity of p53. Cell. 2009; 137:413–431. [PubMed: 19410540]

Watanabe K, Hishiya A. Mouse models of senile osteoporosis. Mol Aspects Med. 2005; 26:221–231. [PubMed: 15811436]

Wu JW, Krawitz AR, Chai J, Li W, Zhang F, Luo K, Shi Y. Structural mechanism of Smad4 recognition by the nuclear oncoprotein Ski: insights on Ski-mediated repression of TGF-beta signaling. Cell. 2002; 111:357–367. [PubMed: 12419246]

Zhu Q, Krakowski AR, Dunham EE, Wang L, Bandyopadhyay A, Berdeaux R, Martin GS, Sun L, Luo K. Dual role of SnoN in mammalian tumorigenesis. Mol Cell Biol. 2007; 27:324–339. [PubMed: 17074815]

Zhu Q, Pearson-White S, Luo K. Requirement for the SnoN oncoprotein in transforming growth factor beta-induced oncogenic transformation of fibroblast cells. Mol Cell Biol. 2005; 25:10731–10744. [PubMed: 16314499]

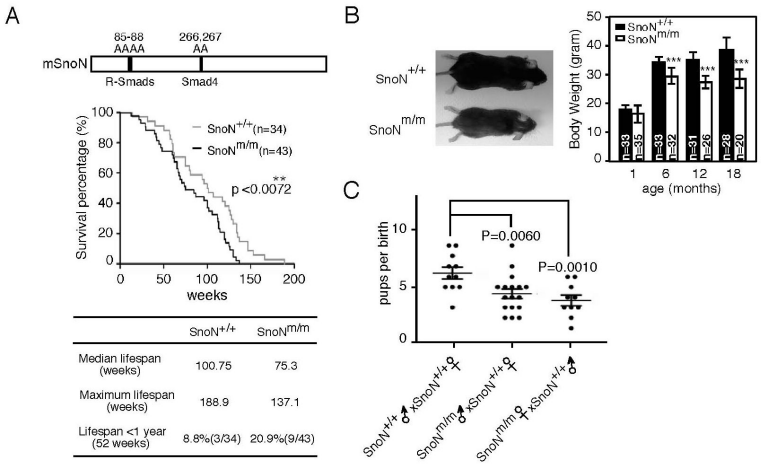

Figure 1. The SnoN$^{m/m}$ mice display shortened lifespan

(A). Top: schematic drawing of mSnoN. Bottom: Kaplan-Meier survival curve and the table below showed a shortened lifespan by the SnoN$^{m/m}$ mice. n=34 for SnoN$^{+/+}$ mice; n=43 for SnoN$^{m/m}$ mice. p<0.0072. **(B).** The SnoN$^{m/m}$ mice were smaller. Top: 18-month old SnoN$^{+/+}$ and SnoN$^{m/m}$ littermates are shown. Bottom: body weight analysis. The SnoN$^{m/m}$ mice stopped gaining weight after 6-month old (P<0.0001). **(C).** The SnoN$^{m/m}$ mice exhibited reduced litter size. The mean litter size was analyzed during a 6-month period of breeding between WT parents (SnoN$^{+/+}$ × SnoN$^{+/+}$: 5 pairs) and WT/homozygous parents (SnoN$^{m/m}$ male × SnoN$^{+/+}$ female: 6 pairs or SnoN$^{m/m}$ female × SnoN$^{+/+}$ male: 5 pairs). The three groups were age-matched first time parents. Both male and female SnoN$^{m/m}$ mice displayed a reduced litter size (male: 4.4 p=0.0060; female: 3.7, p=0.0010) compared to SnoN$^{+/+}$ controls (6.4).

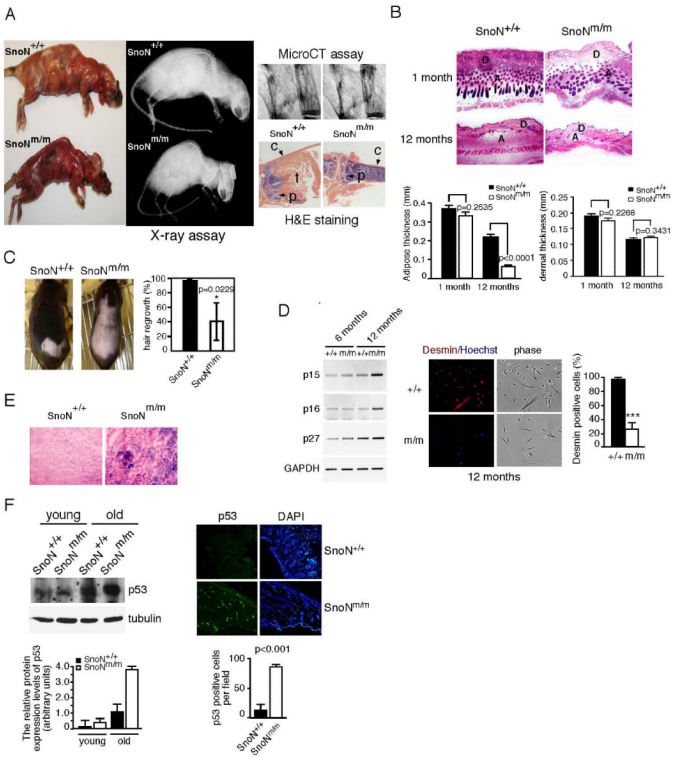

Figure 2. The SnoN$^{m/m}$ mice exhibit osteoporosis and other aging phenotypes

(A). 18 month-old SnoN$^{m/m}$ mouse displayed reduced muscle mass, decreased subcutaneous fat and kyphosis (dotted line, left panel). Whole-mount X-ray (middle) and MicroCT (top right) analyses detected decreased bone density in tail, limbs and spinal cord regions in SnoN$^{m/m}$ mice. Lower right panels: H&E stain of cross sections of tibias from 18 month-old SnoN$^{+/+}$ (left) and SnoN$^{m/m}$ (right) mice. Note the reduction in cortical bone thickness (c, arrow) and the absence of trabecular bone (t) in the tibia of the SnoN$^{m/m}$ mouse. P: epiphyseal plate. **(B).** H&E stain of dorsal skin from a 12-month-old SnoN$^{m/m}$ mouse (right) showed near absence of subcutaneous adipose layer when compared to that of the SnoN$^{+/+}$ (left) mouse. d: dermis; a: subcutaneous adipose tissue. Data from three sets of H&E sections per mouse, and 2 pairs of mice for each age group were quantified (bottom). **(C).** Reduced hair regrowth in 12-month-old SnoN$^{m/m}$ mice. The shaved area is indicated by the red dotted line. Pictures were taken 30 days after shaving. Mean hair regrowth was scored with a transparent grid and show in the graph (P=0.0229, n=3). Data are presented as mean ±SD. **(D)** Left: satellite cells isolated from the injuried 12-month old SnoN$^{m/m}$ mice expressed a higher level of p15, p16 and p27. RNA was extracted from satellite cells prepared from 6- or 12-month-old mice and subjected to RT-PCR analysis. Right: Myogenic differentiation of SnoN$^{m/m}$ satellite cells (m/m) or WT satellite cells (+/+) in culture was monitored by the expression of myogenic marker desmin (red), and myotube formation (phase contrast, middle) and quantified. Data represents means ± S.E.M from four images for each cell type in two different experiments ($p<0.001$). **(E).** Cryostat sections from the skin of 18-month-old SnoN$^{+/+}$ and SnoN$^{m/m}$ mice were stained for SA-β-gal. **(F).** Left: p53 levels in 4- or 18-month-old mice by western blotting. p53 expression was normalized to tubulin and quantified (bottom). Right: Representative equatorial microscopic images of skin sections from 18-month-old mice stained with anti-p53. The number of p53 postive cells per field was quantified and shown below. Data represents means ± S.E.M from 4 images per sample in two different experiments ($p<0.001$).

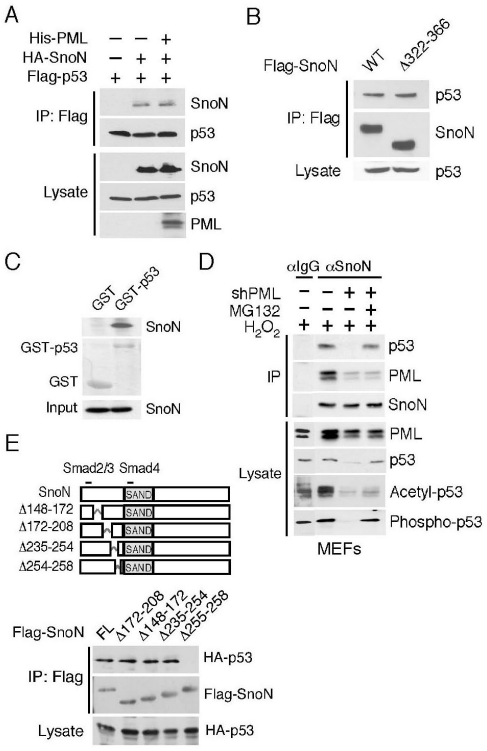

Figure 3. SnoN directly binds to p53

(A). Flag-p53 and HA-SnoN were transfected together with or without His-PML into 293T cells. SnoN that associated with p53 was isolated by immunoprecipitation with anti-Flag and detected by western blotting with anti-HA. (**B).** PML is not required for the SnoN-p53 interaction. Flag-tagged WT SnoN or SnoN(Δ322-366) defective in PML binding was co-transfected with HA-p53. The SnoN-p53 interaction was measured as described in (**A**). (**C).** Bacterial expressed recombinant GST-p53 or GST was incubated with recombinant SnoN (bottom) in a GST-pull down assay. GST-p53-bound SnoN was detected by western blotting with anti-SnoN (top). The amounts of input GST-p53 and GST were shown by Coomassie staining (middle panel). (**D).** Endogenous SnoN and p53 interact in MEF. Primary MEFs infected with a retrovirus expressing shPML or vector control were treated with 80 μM of H_2O_2 for 24 hrs (to induce p53) or 10 μM of MG132 or DMSO for 5 hrs as indicated. Endogenous p53 and PML associated with SnoN were isolated by immunoprecipitation with anti-SnoN and detected by western blotting with anti-p53 or anti-PML. (**E)**. Top: Schematic drawing of SnoN mutants. Bottom: Residues 255-258 in SnoN is required for binding to p53. Interaction between Flag-tagged WT or mutant SnoN with HA-p53 was analyzed as described above.

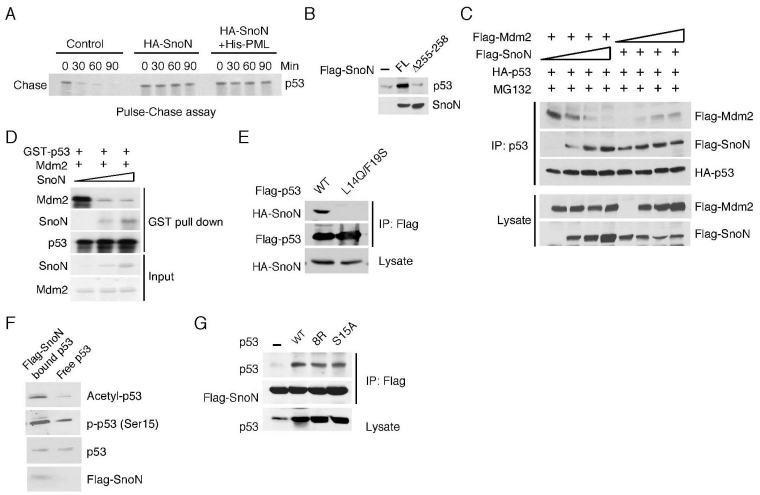

Figure 4. SnoN induces stabilization and activation of p53

(A). Pulse-chase assay. 293T cells transfected with Flag-p53 with or without HA-SnoN or HA-SnoN plus His-PML were pulse-labeled with ^{35}S-express and chased for the indicated time. ^{35}S-labeled p53 was isolated by immunoprecipiation and detected by autoradiography. SnoN-bound p53 showed a significant longer half-life. (**B).** Stabilization of p53 requires a direct SnoN-p53 interaction. Flag-p53 was cotransfected with WT or SnoN Δ255-258. The levels of p53 expression were measured by western blotting with anti-Flag. (**C).** SnoN can compete with Mdm2 for binding to p53. 293T cells were transfected with a fixed amount of HA-p53 and Flag-Mdm2 and increasing amounts of Flag-SnoN or fixing amount of Flag-SnoN and increasing amount of Flag-Mdm2 as indicated. Mdm2 and SnoN that associated with p53 were isolated by immunoprecipitation with anti-HA (p53) and detected by western blotting with anti-Flag. (**D)**. Recombinant SnoN competed with Mdm2 for binding to GST-p53 in vitro. GST-p53 immobilized on glutathione sepharose was incubated with fixing amounts of recombinant Mdm2 and increasing amounts of recombinant SnoN. Mdm2 or SnoN that were bound to p53 was analyzed by western blotting with anti-Mdm2 or anti-SnoN. The input amounts of recombinant SnoN and Mdm2 were visualized by Coomassie stain. (**E).** SnoN and Mdm2 may bind to the same residues in p53. Flag tagged WT or mutant p53 (L14Q/F19S) was co-transfected with HA-SnoN into 293T cells, and SnoN-p53 interaction was analyzed by co-immunoprecipitation assay. **(F).** SnoN enhances p53 acetylation and phosphorylation. p53 bound to SnoN was isolated from primary MEF cells expressing Flag-SnoN by immunoprecipitation with anti-Flag, and free p53 was isolated from SnoN-depleted lysates by immunoprecipitation with anti-p53. Acetylation and phosphorylation of these p53 populations were examined by western blotting with anti-acetyl-p53 (K373; K382) or anti-phosph-p53 (Ser15). (**G).** Acetylation or phosphorylation of p53 is not required for its interaction with SnoN. Flag-SnoN was transfected with WT or mutant p53 (8R and S15A). p53 that associated with SnoN was isolated by immunoprecipitation with anti-Flag and detected by western blotting with anti-p53.

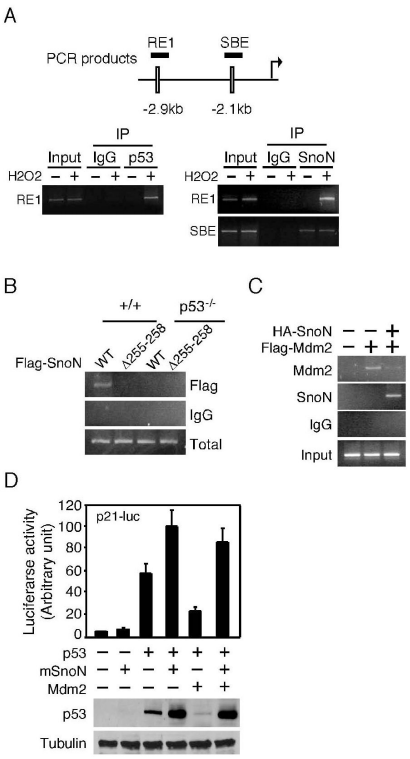

Figure 5. SnoN is recruited to the p53 binding element in the p21 promoter

(A). Top: Schematic drawing of the p53 binding element, RE1 and Smad binding site, SBE in the p21 promoter. The positions of the predicted PCR fragments in the ChIP assay were shown. **Bottom:** Binding of SnoN and p53 to RE1 region is induced by oxidative stress. SnoN (right panels) or p53 (left) bound to the RE1 region was examined by the CHIP assay with anti-SnoN or anti-p53, respectively, in primary MEF cells before or after treatment with H_2O_2. The amount of RE1 fragment in total cell lysate was examined by PCR using the same set of primers as Input. A parallel ChIP assay with anti-IgG was used as a negative control. Lower right panel: SnoN bound to SBE in primary MEF cells before or after treatment with H_2O_2 was analyzed by ChIP using anti-SnoN. (**B**)**.** Recruitment of SnoN to p53 responsive element (RE1) is dependent on its interaction with p53. Flag-tagged WT or SnoNΔ255-258 was transfected into WT or $p53^{-/-}$ MEF. The amount of Flag-SnoN bound to RE1 was analyzed by ChIP with anti-Flag. (**C**)**.** SnoN prevents binding of Mdm2 to the p53 responsive element in the p21 promoter. Flag-Mdm2 were co-tranfected into primary MEF with or without HA-SnoN. Binding of Mdm2 or SnoN to the RE1 region was analyzed by the CHIP assay using anti-Flag or anti-HA respectively. **(D).** SnoN activates p53-dependent transcription by antagonizing Mdm2. $p53^{-/-}$ MEF was transfected with p21-luc together with p53, SnoN and/or Mdm2. Luciferase activities were measured 48 hours after transfection. The expression levels of p53 in the reactions were detected by western blotting.

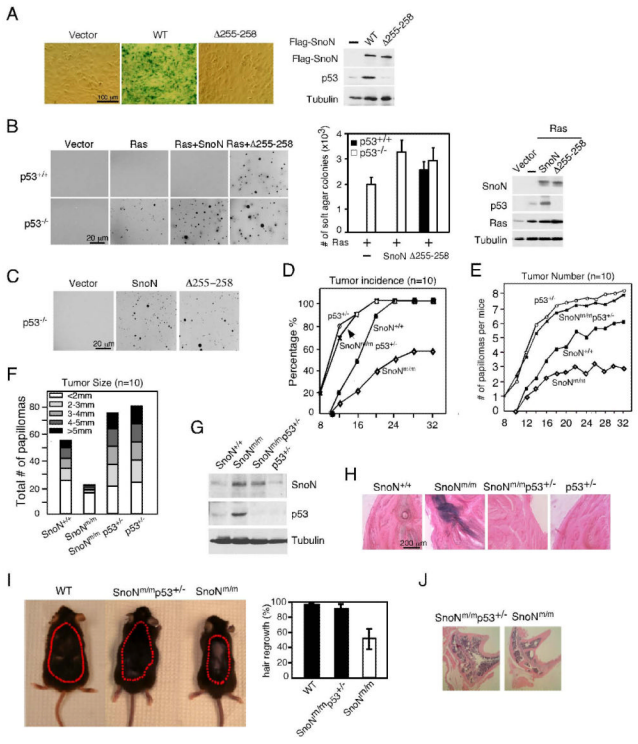

Figure 6. Interactions between SnoN and p53 is required for SnoN-induced senescence and inhibition of oncogene transformation

(A). Primary MEF cells at P3 were infected with retroviruses expressing Flag-tagged WT or mutant SnoN. Senescence of cells was measured by SA-β-gal staining. The levels of p53 and SnoN in these cells were analyzed by western blotting. **(B).** The anti-tumorigenic activity of SnoN is dependent on the SnoN-p53 interaction. WT or $p53^{-/-}$ MEF cells at P3 were infected by retroviruses expressing the constitutively active Ras followed by infection again with retroviruses expressing WT or mutant SnoN or shSnoN. Doubly infected cells were subjected to the soft-agar assay, and the colonies were visualized and quantified. The levels of SnoN, p53 and Ras were detected by western blotting. **(C).** $p53^{-/-}$ MEF cells at P3 were infected with retroviruses expressing WT or mutant SnoN and subjected to the soft-agar assay. (**D**). The two-step skin carcinogenesis protocol was applied to $SnoN^{m/m}p53^{+/-}$, $SnoN^{m/m}$, $p53^{+/-}$, and $SnoN^{+/+}$ mice. The incidence (**D**), average number (**E**) and sizes (**F**) of tumors developed within the 30-week window were recorded and shown in the graphs (n=10 mice for each group). (**G**). Tumors from the $SnoN^{m/m}$ mice displayed elevated p53. The expression of p53 and SnoN in tumor samples was assessed by western blotting with anti-p53 or anti-SnoN. (**H**). Senescence is detected in tumors derived from the $SnoN^{m/m}$ mice. Tumors of 2mm in diameter were collected from various mouse lines and stained for SA-β-gal. **(I).** The defective hair regrowth activity in $SnoN^{m/m}$ mice was rescued in 12-month-old $SnoN^{m/m}p53^{+/-}$ mice. The shaved area is indicated by the red dotted line. Pictures were taken 30 days after shaving. Mean hair regrowth was scored with a transparent grid and show in the graph (n=3). Data are presented as mean±SD. **(J).** $SnoN^{m/m}p53^{+/-}$ mice displayed a markedly increased bone thickness. Cross sections of tibias from 12 month-old $SnoN^{m/m}p53^{+/-}$ (left) and $SnoN^{m/m}$ (right) mice.